

Fatigue behavior of circular hollow tube and wood filled circular hollow steel tube

Ravindra R. Malagi^a and Bharatesh A. Danawade^{*}

Department of PDM, Visvesvaraya Technological University, Belgaum, 590 014, India

(Received February 09, 2014, Revised January 16, 2015, Accepted February 03, 2015)

Abstract. This paper presents the experimental work on fatigue life and specific fatigue strength of circular hollow sectioned steel tube and wood filled circular hollow section steel tube. Burning effect was observed in the case of circular hollow sectioned steel tube when it is subjected to Maximum bending moment of 19613.30 N-mm at 4200 rpm, but this did not happen in the case of wood filled hollow section. Statistical analysis was done based on the experimental data and relations have been built to predict the number of cycles for the applied stress or vice versa. The relations built in this paper can safely be applied for design of the fatigue life or fatigue strength of circular hollow sections and wood filled hollow sections. Results were validated by static specific bending strengths determined by ANSYS using a known applied load.

Keywords: stiffness; fatigue life; specific fatigue strength; reversed cycle stress; S-N curve

1. Introduction

Fatigue has a strong effect on the stiffness of a composite material. The steel retains its most of the stiffness for its major span of life but after then it drops suddenly. Composite materials typically have a longer fatigue life compared to steel and give warning that it is losing its stiffness. These characteristics of composites can be used advantageously for structural applications. Fatigue is among the most common cause of failure of circular cross sectioned shafts used for power transmission. ASM (1975) states that fatigue failures start at the most vulnerable point in dynamically stressed area. The vulnerable point may be mechanical or metallurgical or combination of the two. Bao *et al.* (1996) investigated fatigue behavior of several wood composites for determining the allowable design stress. da Fonte and de Freitas (1999) presents that the shafts run with steady torsion load superimposed with bending stress fail either due to shaft self weight or possible misalignment. Berndt and Van Bennekorn (2001) conclude that in spite of the preventive measures fatigue failure can still occur due to defects introduced during fabrication and/or degradation of shafts during service. Bhaumik *et al.* (2002) presented a case

^{*}Corresponding author, Ph.D. Student, E-mail: bharatesh23@gmail.com

^a Professor, E-mail: rrmalagi@rediffmail.com

study on fatigue failure of hollow power transmission shaft. An analysis of the failure, together with recommendations for failure prevention is presented. The paper recommends use of cleaner material, minimization of stress concentration, and better surface finish to avoid fatigue failure. Schneider and Maddox (2003) presented best practice guide on statistical analysis of fatigue data. Miscow *et al.* (2004) designed and built fatigue simulator to test full-scale drill pipes under rotating cycling bending and constant tension loading. The fundamental fatigue mechanisms were investigated via laboratory tests in small samples. The fatigue life curve was obtained for drill pipe API S-135 grade steel from small scale tests. The full size drill pipe test results are coherent with experimental procedures. West System Inc. (2005) catalogue on fatigue explains that wood exhibits unusually good fatigue resistance although its static one time load strength is not high. Chen *et al.* (2006) conducted low cycle fatigue tests to predict fatigue life of 304 stainless steel tubular geometry with an outer diameter of 12.5 mm and an inner diameter of 10 mm. The fatigue loading applied to the specimen was tension-compression followed by torsion. A damage model considers the effect of non-proportionality in loading due to loading mode changes is proposed.

Dawood *et al.* (2007) investigated the steel-concrete bridge beams strengthened with high modulus carbon fiber reinforced polymer under the overloading and fatigue conditions. Kim and Heffernan (2008) presented progress and achievement in the application of FRP on strengthening reinforced concrete beams subjected to fatigue. Mahagaonkar *et al.* (2009) Examines the effect of process parameters such as pressure, shot size, nozzle distance and the exposure time on the fatigue performance of AISI 045 and 316L material. Expressions correlating fatigue life and the process parameters for both materials were developed, which are useful in predicting fatigue life. Zhu *et al.* (2009) conducted field applications and laboratory research which shows the feasibility of concrete-filled fiber reinforced polymer tube in bridges. An Analytical tool is developed to trace the response of CFFTs under fatigue loading. A detailed parametric study shows that fatigue response of CFFT beams can improve by either increasing the reinforcement index or the effective modulus of FRP tube in the longitudinal direction. Yavari *et al.* (2010) report increase in fatigue life of fiberglass/epoxy composites with various weight fractions of graphene platelets. Roeder *et al.* (2010) presents that concrete infill confined in steel tube delays local and global buckling of the tube. CFT's provide significant resistance in shear, compression and bending. Amiri (2010) carried experimental and theoretical study to investigate temperature evolution of aluminum 6061 and stainless steel 304 specimens subjected to cyclic fatigue using thermographic technique. Results reveal that surface temperature of specimens can be directly related to number of cycles to failure.

Wood shows their inherent ability to withstand high cyclic wind loads year after year. This ability of wood is developed by nature for dynamic and adverse environment. Hence specific strength and stiffness of woods is greater than metals. When such a wood is used in building composite system for fatigue loads naturally life and strength of composite gives better results than individual metals. Very little information is available on the fatigue behavior and properties of circular hollow sectioned tubes and circular wood filled hollow sections. In this laboratory level work 4-point rotating bending fatigue testing machine was used to determine the fatigue strength and fatigue life. On this machine specimens were subjected to completely reversed stress cycles with constant amplitude and results were presented and discussed. A statistical approach for predicting the specific strength and fatigue life is given. An attempt has been made to use finite element analysis using ANSYS to determine the properties of wood filled tubes using static tests conditions. The results of all tests are compared and found to be coherent.

2. Materials

Two types of specimens were used for study: (i) Circular Hollow Section Steel Tube; (ii) Teak Wood Filled Circular Hollow Sectioned Steel Tube. Carbon steel material was used for circular hollow sectioned tube and teak wood was used as the filling material. The reasons for selecting teak wood as filler material; it is bench mark material from wood species, renewable, sustainable, machinable, non-corrosive, durable, light in weight. The carbon steel is generally used steel material for construction of wide range of construction and engineering applications. Both the materials are procured from local market and desirable material properties were obtained experimentally and compared with available research data. The carbon steel properties were determined experimentally as per the ASTM E8 (2011) are as follows yield stress, Tensile stress and Young's modulus are 311.46 MPa, 446.18 MPa, and 212.48 GPa with a standard deviation of 1.65, 3.36 and 2.40 respectively. Poisson's ratio of steel tube is taken as 0.29.

Teakwood longitudinal modulus of elasticity properties were determined experimentally as per ASTM D143 (1994) and was 11854.89 MPa with standard deviation of 687.2, Poisson's ratio was 0.52 was determined as per the procedure discussed by Danawade *et al.* (2013).

Carbon steel specimens were prepared on precision lathe by skilled operator and polished to maintain the dimensions and tolerances. Teak wood specimens were prepared on lathe to the size to fit in to the circular hollow section of the steel tube. The solid circular teak wood is fitted in to the circular hollow sectioned steel tube using light to medium interference fit to produce the composite using suitable hydraulic press. Allowable interference is designed based on the functional requirements of solid teakwood shaft and a steel tube. Allowable interference between solid teakwood and steel tube is determined using following formula adopted from design guide manual 1 of DuPont Engineering Polymers

$$I = \sigma * \frac{do}{W} [(W + vs)/Es + (1 - vw)/Ew] \quad (1)$$

$$\text{Where } W = \frac{(do^2 + dw^2)}{(do^2 - dw^2)}$$

Measured value of inside diameter of steel tube is taken as basic size and allowable interference value added to obtain maximum size of teak wood for desired interference. Residual stresses induced in circular hollow steel tube and teak wood shaft due to interference fit were calculated using following Eq. (2) from Shigley *et al.* (2004) on press and shrink fit

$$P = \frac{1}{Ks + Kw} * \frac{I}{ri} \quad (2)$$

$$\text{Where } Ks = (1/Es) \left[\frac{ro^2 + ri^2}{ro^2 - ri^2} \right] \text{ and } Kw = \left(\frac{1}{Ew} \right) [1 - vw]$$

Teakwood experiences an external pressure resulting in compressive tangential and radial stresses and are given by Eq. (3)

$$\sigma_{wt} = \sigma_{wr} = -P \quad (3)$$

Steel tube experiences internal pressure resulting in tensile tangential stress given by Eq. (4) and compressive radial stress and are given by Eq. (5)

$$\sigma_{st} = P * [(ro^2 + ri^2)/(ro^2 - ri^2)] \quad (4)$$

$$\sigma_{sr} = -P \quad (5)$$

The allowable interference and stresses developed in steel tube and teak wood are shown in

Table 1 Allowable interference and stress developed due to interference

Specimen code	d_o , mm	d_i , mm	W	I , mm	d_w , mm	P , Mpa	$\sigma_{wt}, \sigma_{wr},$ σ_{sr} , Mpa	σ_{st} , Mpa
WFCHS_200_1	10.94	8.75	4.55	0.05	8.80	168.84	-168.84	786.82
WFCHS_200_2	10.92	8.64	4.35	0.05	8.69	178.67	-178.67	795.28
WFCHS_200_3	10.93	8.69	4.44	0.05	8.74	174.24	-174.24	791.47
WFCHS_175_1	10.96	8.55	4.11	0.05	8.60	191.74	-191.74	806.44
WFCHS_175_2	10.93	8.60	4.25	0.05	8.65	183.78	-183.78	799.65
WFCHS_175_3	10.94	8.57	4.18	0.05	8.62	187.86	-187.86	803.14
WFCHS_150_1	10.99	9.06	5.24	0.04	9.10	142.14	-142.14	763.63
WFCHS_150_2	10.95	8.86	4.79	0.05	8.91	158.48	-158.48	777.87
WFCHS_150_3	10.97	8.96	5.01	0.04	9.00	150.20	-150.20	770.67
WFCHS_125_1	11.00	8.71	4.36	0.05	8.76	177.97	-177.97	794.67
WFCHS_125_2	10.93	8.80	4.69	0.05	8.85	162.90	-162.90	781.70
WFCHS_125_3	10.96	8.75	4.52	0.05	8.80	170.49	-170.49	788.24
AVG	10.95	8.75	4.54	0.05	8.79	170.61	-170.61	788.30
SD	0.03	0.16	0.34	0.00	0.15	15.03	15.03	12.97



Fig. 1 Semi finished specimens of CHS and teak wood

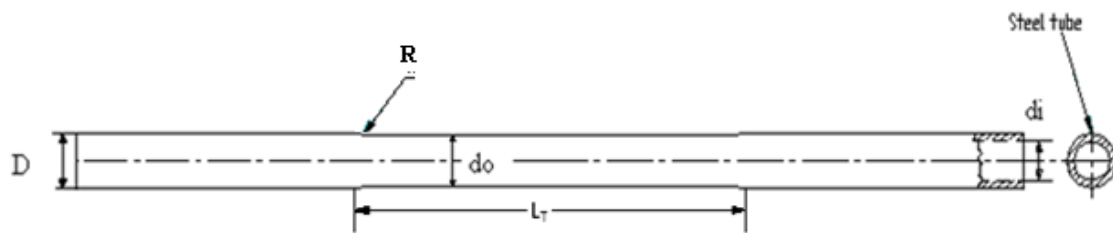


Fig. 2 Nomenclature of steel tube specimen

Table 1.

The semi finished specimens ready for finishing and assembly are shown in Fig. 1.

The dimensions of both steel and the composite specimens were decided considering the loading diameter and length of available standard fatigue testing machine by Fine Testing Machine (2008) which meets the requirement of IS 5075:1969 standard. The nomenclature of steel tube specimens are as shown in Fig. 2.

Table 2 Geometrical and physical properties of CHS

Specimen code	D , mm	d_o , mm	d_i , mm	Lt , mm	Lp , mm	L , mm	R , mm	ρ , kg/m ³	I_i , mm ⁴
CHS_200_1	12.02	10.98	8.75	96	72	260	30	7406.62	425.73
CHS_200_2	12.00	10.99	8.64	96	72	260	30	7698.92	442.54
CHS_200_3	12.01	10.98	8.69	96	72	260	30	7542.52	433.55
CHS_175_1	12.03	10.88	8.55	96	72	260	30	6949.19	425.52
CHS_175_2	12.03	11.06	8.60	96	72	260	30	7610.12	465.99
CHS_175_3	12.03	10.97	8.57	96	72	260	30	7285.29	446.10
CHS_150_1	12.01	11.05	9.06	96	72	260	30	7394.38	401.11
CHS_150_2	12.02	11.03	8.86	96	72	260	30	7817.78	424.08
CHS_150_3	12.01	11.04	8.96	96	72	260	30	7610.37	412.82
CHS_125_1	11.99	10.98	8.71	96	72	260	30	7211.10	430.96
CHS_125_2	12.05	11.12	8.80	96	72	260	30	7633.28	456.19
CHS_125_3	12.02	11.05	8.75	96	72	260	30	7431.02	444.10
AVG	12.02	11.01	8.75	96	72	260	30	7465.88	434.06
SD	0.02	0.06	0.15	0.00	0.00	0.00	0.00	228.77	17.36

Table 3 Geometrical and physical properties of teak wood filled circular hollow sections

Specimen code	D , mm	d_o , mm	Lt , mm	Lp , mm	L , mm	R , mm	ρ , kg/m ³	I_i , mm ⁴
WFCHS_200_1	12.03	10.94	96	72	260	30	3653.40	703.14
WFCHS_200_2	11.99	10.92	96	72	260	30	3626.76	698.01
WFCHS_200_3	12.01	10.93	96	72	260	30	3640.06	700.57
WFCHS_175_1	12.1	10.96	96	72	260	30	3387.42	708.29
WFCHS_175_2	12.02	10.93	96	72	260	30	3350.48	700.57
WFCHS_175_3	12.06	10.94	96	72	260	30	3362.76	703.14
WFCHS_150_1	12.06	10.99	96	72	260	30	3374.73	716.08
WFCHS_150_2	12	10.95	96	72	260	30	3325.86	705.71
WFCHS_150_3	12.03	10.97	96	72	260	30	3350.23	710.88
WFCHS_125_1	11.95	11.00	96	72	260	30	3362.58	718.69
WFCHS_125_2	12.04	10.93	96	72	260	30	3277.80	700.57
WFCHS_125_3	11.99	10.96	96	72	260	30	3313.94	708.29
AVG	12.02	10.95	96.00	72.00	260.00	30.00	3418.84	706.16
SD	0.04	0.02	0.00	0.00	0.00	0.00	130.81	6.23

The detailed geometrical properties of circular hollow sectioned tubes are shown in Table 2.

The teak wood filled circular hollow sectioned steel tube ready for polishing are shown in Fig. 3, and geometrical properties of specimens are shown in Table 3.

3. Methods of investigation

3.1 Experimental

In this work 4-point rotating bending fatigue testing machine was used to determine the fatigue strength and fatigue life. On this machine specimen is subjected to completely reversed stress cycles with constant amplitude. During each cycle, the rotating specimen is subjected to both tensile and compressive stresses alternatively. The schematic rotating bending fatigue testing machines specimen loading arrangement is shown in the Fig. 3.

The fatigue behavior of circular hollow sectioned steel tube and Teak wood filled steel tube is determined by conducting laboratory tests on a 24 number of polished specimens. A single test consists of applying a known, constant bending load on a rotating specimen. During the one cycle of rotation, the specimen is subjected to the two types of bending stresses (tensile and compressive) having same magnitude but opposite signs and due to these alternative stresses the specimen fails after certain number of cycles. The number of cycles sustained by the specimen up to the failure is recorded by the counter. The above procedure is repeated for all the specimens by applying different bending moments at constant spindle rpm. The number of cycles sustained by each specimen up to the failure is recorded.

The specimens were first subjected to maximum bending moment of 200 kg-cm. The bending moment is reduced by 25 kg-cm in each step and number of cycles to failure was noted. The results obtained were plotted to generate S-N curve for both steel and wood-steel composite material.

The bending strength and specific bending strength were calculated using following relations.

$$I_i = \pi/64(d_o^4 - d_i^4) \quad (6)$$

$$\frac{M}{I_i} = \frac{\sigma b}{y} = \frac{E}{R} \quad (7)$$

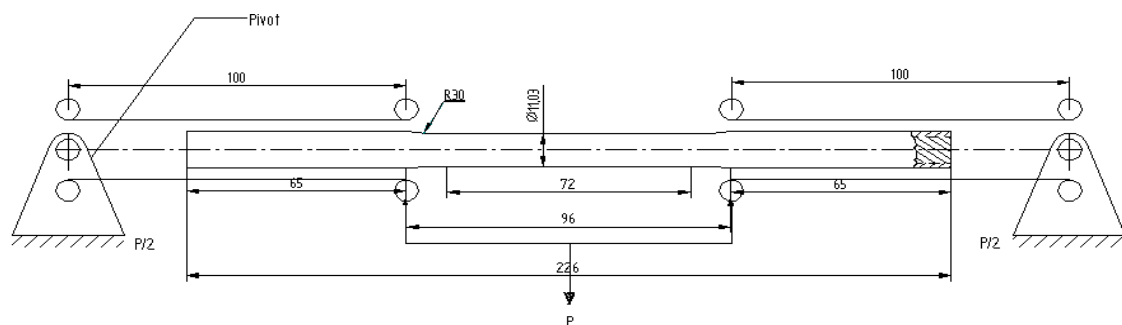


Fig. 3 Specimen loading arrangement, Fine testing machine (2008)

$$M = \frac{FLs}{2} \tag{8}$$

$$Se = \frac{\sigma b}{\rho} \tag{9}$$

The experimented data for circular hollow sectioned steel tube is presented in Table 4.

When circular hollow sectioned steel tubes were tested for bending moment of 19613.30 N-mm the burning effect was observed. This effect was not observed for other values of bending moment. The burning was due to severe combined loading of specimen which was subjected to tensile-compression and torsional. Fig. 4 shows the burning effect of specimens.

All the specimens failed due to crack initiation on the surface of the specimen and propagation of the crack ending in failure. The crack initiation and nature of failure is same in all failed components and the failure is as shown Fig. 5.

The experimented data for teak wood filled circular hollow sectioned steel tube is presented in Table 5.

Table 4 Experimental data of CHS specimens

Specimen Code	M, N-mm	N, rpm	Nf	σb, Mpa	Se, Mpa-m ³ /kg
CHS_200_1	19613.30	4200	27175	252.92	0.0341
CHS_200_2	19613.30	4200	19420	243.54	0.0316
CHS_200_3	19613.30	4200	23296	248.36	0.0329
CHS_175_1	17161.63	4200	279374	219.40	0.0316
CHS_175_2	17161.63	4200	262611	203.66	0.0268
CHS_175_3	17161.63	4200	270991	211.01	0.0290
CHS_150_1	14709.97	4200	3653300	202.62	0.0274
CHS_150_2	14709.97	4200	3434102	191.30	0.0245
CHS_150_3	14709.97	4200	3543701	196.69	0.0258
CHS_125_1*	12258.31	4200	483848636	156.16	0.0217
CHS_125_2*	12258.31	4200	423364071	149.40	0.0196
CHS_125_3	12258.31	4200	362883332	152.50	0.0205

*specimens did not fail



Fig. 4 Burning effect of CHS at maximum bending moment Fig. 5 Crack initiation and nature of failure

Table 5 Experimental data for WFCHS specimens

Specimen Code	M , N-mm	N , rpm	N_f	σ_b , Mpa	Se , Mpa-m ³ /kg
WFCHS_200_1	19613.30	4200	168840	152.58	0.0418
WFCHS_200_2	19613.30	4200	157245	153.42	0.0423
WFCHS_200_3	19613.30	4200	145650	153.00	0.0420
WFCHS_175_1	17161.63	4200	1533000	132.78	0.0392
WFCHS_175_2	17161.63	4200	1628188	133.87	0.0400
WFCHS_175_3	17161.63	4200	1680594	133.51	0.0397
WFCHS_150_1	14709.97	4200	18982273	112.88	0.0334
WFCHS_150_2	14709.97	4200	18063376	114.12	0.0343
WFCHS_150_3	14709.97	4200	17901170	113.50	0.0339
WFCHS_125_1*	12258.31	4200	462873117	93.81	0.0279
WFCHS_125_2	12258.31	4200	414364288	95.62	0.0292
WFCHS_125_3*	12258.31	4200	485848656	94.84	0.0286

*' specimens did not fail



Fig. 6 Fatigue failure of WFCHS

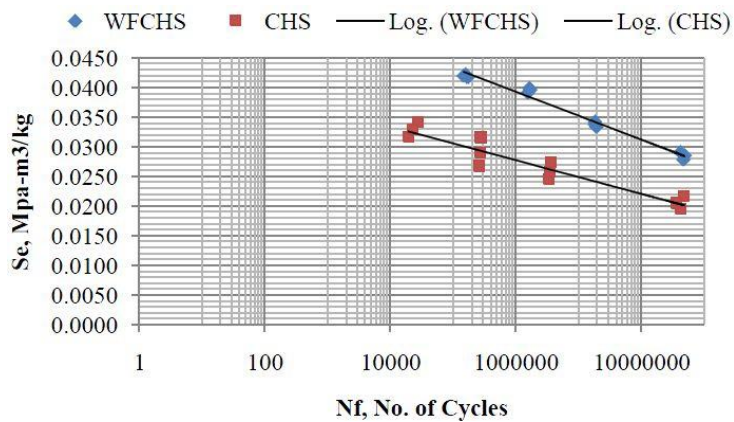


Fig. 7 Comparison of SN curve

Table 6 Averaged experimental data of CHS for log curve

Specimen code	N_f	S_e , Mpa-m ³ /kg	$LN(N_f)$	$LN(S_e)$
CHS_200	23297	0.0329	10.06	-3.4142
CHS_175	270992	0.0291	12.51	-3.5370
CHS_150	3543701	0.0259	15.08	-3.6533
CHS_125	423365346	0.0206	19.86	-3.8833

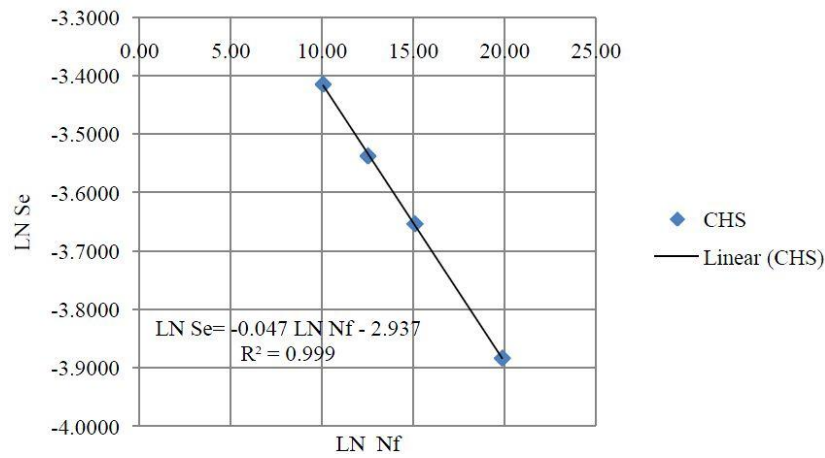


Fig. 8 LN Se V/s LN Nf curve for CHS

Table 7 Comparison of experimental and statistical values of specific fatigue strength of CHS

Specimen code	N_f	S_e , Mpa-m ³ /kg	$LN(N_f)$	$LN(S_e)$	$LN(S_s)$	S_s , Mpa-m ³ /kg	S_s/S_e
CHS_200_1	27175	0.0341	10.21	-3.3771	-3.4169	0.0328	0.96
CHS_200_2	19420	0.0316	9.87	-3.4536	-3.4011	0.0333	1.05
CHS_200_3	23296	0.0329	10.06	-3.4134	-3.4096	0.0331	1.00
CHS_175_1	279374	0.0316	12.54	-3.4555	-3.5264	0.0294	0.93
CHS_175_2	262611	0.0268	12.48	-3.6208	-3.5235	0.0295	1.10
CHS_175_3	270991	0.0290	12.51	-3.5417	-3.5250	0.0295	1.02
CHS_150_1	3653300	0.0274	15.11	-3.5971	-3.6472	0.0261	0.95
CHS_150_2	3434102	0.0245	15.05	-3.7103	-3.6443	0.0261	1.07
CHS_150_3	3543701	0.0258	15.08	-3.6556	-3.6458	0.0261	1.01
CHS_125_1	483848636	0.0217	20.00	-3.8325	-3.8769	0.0207	0.96
CHS_125_2	423364071	0.0196	19.86	-3.9336	-3.8706	0.0208	1.07
CHS_125_3	362883332	0.0205	19.71	-3.8862	-3.8634	0.0210	1.02
AVG							1.01
SD							0.05

Comparison of SN curve of circular hollow sectioned tube and wood filled circular hollow sectioned tube is shown in Fig. 7.

3.2 Statistical analysis

The SN curves for CHS are drawn using mean of the experimental values with the aid of Microsoft office excel tool and results were fitted by logarithmic options. The relations and goodness of fit (R^2) were obtained. The value so obtained is shown in Table 6 and SN curve is shown in Fig. 8. The relation between the fatigue life and fatigue strength is given by Eq. (5).

$$\ln Ss = -0.047 \ln Nf - 2.937 \tag{10}$$

The comparison of experimented data and statistical data of fatigue strength of CHS specimens is presented in Table 7.

The SN curves for WFCHS are obtained as using the same procedure discussed for CHS sample and the values so obtained are shown in Table 8 and SN curve is shown in Fig. 8. The relation between the fatigue life and fatigue strength is given by Eq. (6).

$$\ln Ss = -0.050 \ln Nf - 2.534 \tag{11}$$

Table 8 Averaged experimental data of CHS for log curve

Specimen code	N_f	$Se, \text{Mpa}\cdot\text{m}^3/\text{kg}$	$LN(N_f)$	$LN(Se)$
WFCHS_200	157245	0.0420	11.97	-3.1693
WFCHS_175	1613927	0.0396	14.29	-3.2285
WFCHS_150	18315606	0.0339	16.72	-3.3849
WFCHS_125*	454362020	0.0286	19.93	-3.5556

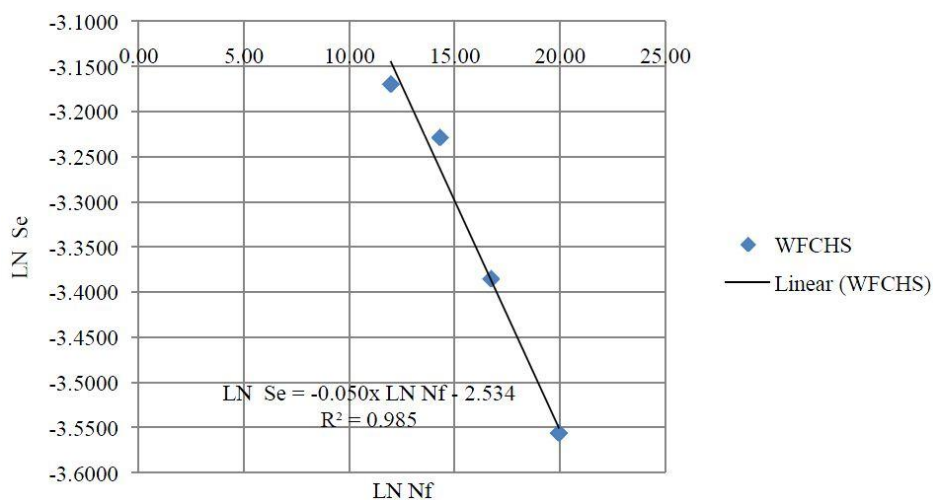


Fig. 9 $LN Se$ V/s $LN Nf$ curve for WFCHS samples

Table 9 Comparison of experimental and statistical values of specific fatigue strength of WFCHS specimens

Specimen code	N_f	S_e , Mpa-m ³ /kg	$LN(N_f)$	$LN(S_e)$	$LN(S_s)$	S_s , Mpa-m ³ /kg	S_s/S_e
WFCHS_200_1	168840	0.0418	12.04	-3.1757	-3.1358	0.0435	1.04
WFCHS_200_2	157245	0.0423	11.97	-3.1629	-3.1323	0.0436	1.03
WFCHS_200_3	145650	0.0420	11.89	-3.1693	-3.1284	0.0438	1.04
WFCHS_175_1	1533000	0.0392	14.24	-3.2391	-3.2461	0.0389	0.99
WFCHS_175_2	1628188	0.0400	14.30	-3.2200	-3.2491	0.0388	0.97
WFCHS_175_3	1680594	0.0397	14.33	-3.2264	-3.2507	0.0387	0.98
WFCHS_150_1	18982273	0.0334	16.76	-3.3977	-3.3720	0.0343	1.03
WFCHS_150_2	18063376	0.0343	16.71	-3.3722	-3.3695	0.0344	1.00
WFCHS_150_3	17901170	0.0339	16.70	-3.3850	-3.3690	0.0344	1.02
WFCHS_125_1	462873117	0.0279	19.95	-3.5792	-3.5316	0.0293	1.05
WFCHS_125_2	414364288	0.0292	19.84	-3.5345	-3.5261	0.0294	1.01
WFCHS_125_3	485848656	0.0286	20.00	-3.5537	-3.5341	0.0292	1.02
AVG							1.01
SD							0.02

The comparison of experimented data and statistical data of fatigue strength of WFCHS specimens is presented in Table 9.

3.3 Finite element analysis

Maximum applied stress approaches static strength of the specimen and minimum applied stress range approaches fatigue. Hence wood filled circular hollow sectioned steel tube is tested using maximum stress and minimum stress values of experiment to validate the results. This is done by finite element analysis using ANSYS (2010).

The specimen is modeled and the meshing of the wood-steel composite beam is performed by selecting the required mesh attributes by selecting the material model 1 for wood material and material model 2 for steel material. Meshing is done under Tet free mesh by selecting the suitable scale in the form number of divisions. After performing the meshing the next step is to apply the displacement and load on to the model. Selected nodes are fixed by adding the displacement at the required position by selecting the nodes at that area the displacement in the UX, UY and UZ directions. Once the displacement is applied then the required dynamic load is applied at the required area on to the nodes. ANSYS software performs the solution for the current load step by going to the solution window by selecting solves current LS. Once the solution is done the next step is to read and plot the results in general post processor window. In post processing, the fatigue analysis is performed by giving the input in the form by applying the known bending load and the corresponding fatigue stress is obtained and is compared with the stress obtained by experimental fatigue strength. The meshing and constraining of component is shown in Fig. 10 and output stress distribution is shown in Fig. 11. The comparison between the experimental, statistical and ANSYS values of maximum and minimum specific fatigue strength is shown in Table 10 for a sampled specimens.

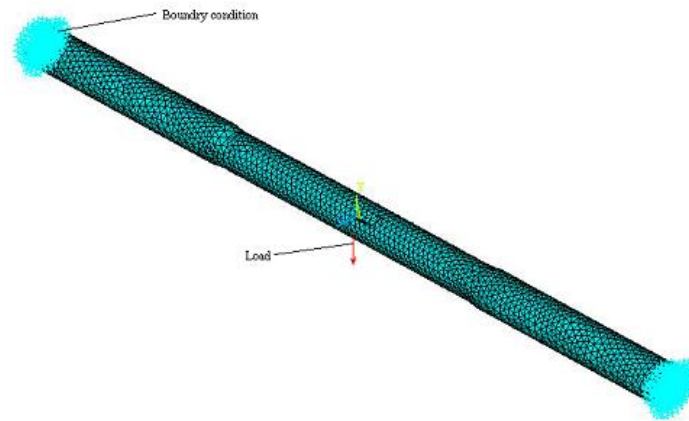


Fig. 10 Meshing of WFCHS specimen

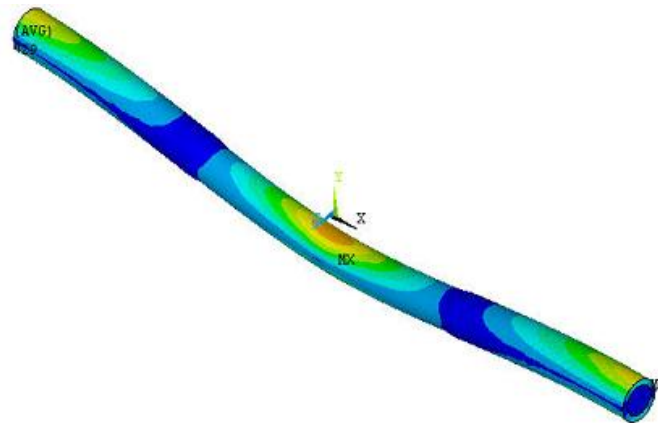


Fig. 11 Out put of ANSYS showing stress distribution

Table 10 Comparison specific strengths of WFCHS

F, N	Se , Mpa-m ³ /kg	Ss , Mpa-m ³ /kg	Sa , Mpa-m ³ /kg	Ss/Se	Sa/Se
392.26	0.0420	0.0435	0.0403	1.04	0.96
245.16	0.0286	0.0292	0.0280	1.02	0.98

4. Conclusions

The experimental investigations carried out show that wood filling in circular hollow sectioned tube enhances the fatigue life considerably. The wood-steel composites specific strength is higher compared to steel. This makes a better alternate material for dynamic loading conditions and alternate material for hollow shafts. The number specimens need to be tested to obtain more accurate results and apply limits of control to the results and use these results to formulate design equations. However statistical analysis done using experimental results gives coherent results even for less number of specimens tested in this investigation. The results of statistical analysis are

higher hence fatigue life can be designed safely using statistical relations designed in this paper.

In the case of circular hollow section tubes burning effect is observed when maximum bending moment is applied. This burning effect in the case of wood filled specimen is not observed. The possible reason for this effect is specimen's poor resistance to combined tensile-compression-torsion loading at the applied load. The effect is not observed for other lower values of stresses.

The specific strength obtained by finite element analysis is lower compared to experimental as well as statistical analysis. The perfect finite element environment needs to be used to obtain comparable results as fatigue being a dynamic test. Further investigations in this regard are necessary to extend this work to real size wood-steel composite shafts.

Acknowledgments

Acknowledge the assistance of Mr. Ghadi Bushan and workshop/laboratory staff of Gharda Institute of Technology, Lavel, Maharashtra, India.

References

- American Society of Metals (1975), Failures of Shafts; Failure Analysis and Prevention, *Metals Handbook*, **10**, 373-397.
- Amiri, M. (2010), "Rapid determination of fatigue failure based on temperature evolution", *Int. J. Fatigue*, **32**(2), 382-389.
- ANSYS (2010), ANSYS Inc., Release 13.0 help.
- ASTM E8 (2011), Standard Test Methods for Tension Testing of Metallic Materials; American Society for Testing of Materials, West Conshohocken, PA, USA.
- ASTM D143 (1994), Standard Method of Testing Small Clear Specimens of Timber; American Society for Testing of Materials, West Conshohocken, PA, USA.
- Bao, Z., Eckelman, C. and Gibson, H. (1996), "Fatigue strength and allowable design stresses for some wood composites used in furniture", *Holz als Roh-und Werkstoff*, **54**(6), 377-382.
- Berndt, F. and Van Bennekorn, A. (2001), "Pump shaft failures-a compendium of case studies", *Eng. Fail. Anal.*, **8**(2), 135-144.
- Bhaumik, S.K., Rangaraju, R., Parameswara, M.A., Venkataswamy, M.A., Bhaskaran, T.A. and Krishnan, R.V. (2002), "Fatigue failure of a hollow power transmission shaft", *Eng. Fail. Anal.*, **9**(4), 457-467.
- Chen, X., Jin, D. and Kim, K.S. (2006), "Fatigue life prediction of type 304 stainless steel under sequential biaxial loading", *Int. J. Fatigue*, **28**(3), 289-299.
- da Fonte, M. and de Freitas, M. (1999), "Stress intensity factors for semi elliptical surface cracks in round bars under bending and torsion", *Int. J. Fatigue*, **21**(5), 457-463.
- Danawade, B., Malagi, R. and Malagi, S. (2013), "Flexural strength properties of teak wood filled rectangular hollow sectioned thin steel tube and its application in automobile", *SAE Technical Paper*, 2013-01-1179.
- Dawood, M. Rizikalla, S. and Summer, E. (2007), "Fatigue and overloading behaviour of steel-concrete composite flexural members strengthened with high modulus CFRP materials", *J. Compos. Construct.*, **11**(6), 659-669.
- DuPont, Design guide manual 1, Dupont Engineering polymers, Reorder No.: H-76838, 70-71.
- Fine Testing Machines (2008), *Product Catalog*, Model FTG-8(D), 2008/163.
- Kim, Y. and Heffernan, P. (2008), "Fatigue behavior of externally strengthened concrete beams with fiber reinforced polymers: State of the art", *J. Compos. Construct.*, **12**(3), 246-256.
- Mahagaonkar, S.B., Brahmankar, P.K. and Seemikeri, C.Y. (2009), "Effect on fatigue performance of shot

- peened components: An analysis using DOE technique”, *Int. J. Fatigue*, **31**(4), 693-702.
- Miscow, G.F., de Miranda, P.E.V., Netto, P.A. and Plácido, J.C.R. (2004), “Techniques to characterize behavior of full size drill pipes and small scale samples”, *Int. J. Fatigue*, **26**(6), 575-584.
- Roeder, C., Lehman, D. and Bishop, E. (2010), “Strength and stiffness of circular concrete filled tubes”, *J. Struct. Eng.*, **136**(12), 1545-1553.
- Schneider, C.R.A. and Maddox, S.J. (2003), “Best practice guide on statistical analysis of fatigue data”, *International Institute of Welding*, IIW-XIII-WG1-114-03.
- Shgley, J.E., Mischke, C.R., Budynas, R.G., Liu, X. and Gao, Z. (2004), *Mechanical Engineering Design*, Tutorial 4-17, *The McGraw Hill*, New York, NY, USA, pp. 1-11.
- West System Inc. (2005), *Fatigue*, Technical Information, Catalog number , 000-545
- Yavari, F., Rafiee, M.A., Rafee, J., Yu, Z.-Z. and Koratkar, N. (2010), “Dramatic increase in fatigue life in hierarchical graphene composites”, *ACS Appl. Mater. Interf.*, **2**(10), 2738-2743.
- Zhu, Z., Ahmad, I. and Mirmiran, A. (2009), “Fatigue modeling of concrete filled fiber reinforced polymer tubes”, *J. Compos. Construct.*, **13**(6), 582-590.

CC

Abbreviations

<i>CHS</i>	Circular hollow section
<i>D</i>	Gripping diameter of tube, mm
<i>d_i</i>	inside diameter of steel tube, mm
<i>d_o</i>	Outsided diameter of steel tube, mm
<i>d_w</i>	Diameter of teak wood shaft, mm
<i>E_s</i>	Young,s modulus of steel, Mpa
<i>E_w</i>	Young,s modulus of teak wood, Mpa
<i>F</i>	Load, N
<i>I</i>	Allowable interference, mm
<i>I_i</i>	Moment of Inertia, mm ⁴
<i>K_s</i>	Design factor for steel tube
<i>K_w</i>	Design factor for teak wood
<i>L</i>	Overall Lentgh of specimen, mm
<i>L_s</i>	Lentgh of beam under consideraion, mm
<i>L_p</i>	Parallel lentgh of specimen, mm
<i>LT</i>	Total lentgh of specimen, mm
<i>M</i>	Bending Moment, N-mm
<i>N</i>	Spindle speed, rpm
<i>N_f</i>	Number cycles
<i>P</i>	Pressure due to interference, Mpa
<i>R</i>	Radius on steel tube, mm
<i>r_i</i>	inside radius of steel tube
<i>r_o</i>	Outside radius of steel tube, mm
<i>S_e</i>	Experimental Specific bending strength
<i>S_s</i>	Statistical specific bending strength
<i>ν_s</i>	Poisson's ration of steel
<i>ν_w</i>	Poisson's ratio of teak wood
<i>W</i>	Design factor for interference
<i>WFCHS</i>	Wood filled circular hollow section
<i>ρ</i>	Density, kg/m ³
<i>σ</i>	Yield stress of steel, Mpa
<i>σ_b</i>	Bending stress, Mpa
<i>σ_{sr}</i>	Compressive radial stress at steel tube, Mpa
<i>σ_{st}</i>	Tensile tangential stress at steel tube, Mpa
<i>σ_{wr}</i>	Radial stress at teak wood, Mpa
<i>σ_{wt}</i>	Compressive tangential stress at teak wood, Mpa